Proceedings of the
International Conference on Mechanical Engineering 2011
(ICME2011) 18- 20 December 2011, Dhaka, Bangladesh

ICME11-RT-023

STRUCTURAL, MAGNETIC AND MAGNETOCALORIC PROPERTIES AT HIGH TEMPERATURE IN $Co_{50}Mn_{30}In_{15}Sn_5$ ALLOY

M. Nazmunnahar[1*], J.J. del Val[1], M. Ilyn[1], L. González[2], J. García[2], J.D. Santos[2], V.M. Prida[2], V. Koledov[3], B. Hernando[2], J. González[1]

[1] Material Physics Dept., Chemistry Fac., Basque Country University, 1072, 20080-San Sebastián, Spain
[2]Departamento de Física, Universidad de Oviedo, Calvo Sotelo s/n, 33007-Oviedo, Spain
[3]Kotelnikov Institute of Radio Engineering and Electronics, RAS, Moscow 125009, Russia

ABSTRACT

In this work we report on microstructural and magnetic characterization of $Co_{50}Mn_{30}In_{15}Sn_5$ alloy melt-spun ribbons in its as-cast state and after being annealing at 923K during 5h. Microstructure was analysed by means of differential scanning calorimetry (DSC) and X-ray diffraction (XRD) techniques, while magnetic measurements (hysteresis loop and magnetization) were performed in the temperature range 1.8 – 1000 K. XRD measurements confirm the presence of Heusler phase Co_2MnSn in the annealed material with crystallites sizing around 33 nm. Ferromagnetic ordering temperatures in Co-based Heusler systems (Co_2MnIn) are considerably higher than in the corresponding Ni_2MnIn ones . In this case, T_C = 450K for the annealed sample is lower than the corresponding one (T_C = 720K) for the as-cast ribbon at 1.2 kOe applied magnetic field. ZFC, FC and FH curve conformed the two well distinct curie temperatures at around 500 K and 720 K respectively. MCE has been evaluated and the maximum value of entropy change is 2.37 $JKg^{-1}K^{-1}$ have been found, which is the same order of magnitude that reported of *Gd* alloys.

Keywords: Melt-Spun Ribbon, Heusler Phase, Recrystallization, Magnetization, Coercivity, Magnetocalo Effect.

1.INTRODUCTION

Magnetic refrigeration which is based on the magnetocaloric effect (MCE) is one of the more relevant topics in the scientific research owing to its very important technological applications, which derive from the attempts made to replace the gas refrigerating technology involving a low impact in the environment and an expected higher energetic efficiency. MCE or adiabatic temperature change is defined as the intrinsic property of the magnetic materials which is expressed by its variation under the action of an external magnetic field which means that MCE is the temperature change of a magnetic material due to the application of a magnetic field[1,2]. This effect results to be more relevant in the vicinity of the Curie Temperature (T_c) where the change of entropy ascribed to the magnetic disorder is usually higher because of the thermal agitation.

It is well known that a material that exhibits a considerable MCE at room temperature is Gd, its problem that requires a high purity, leading to high costs. However, the Co series of Heusler alloys have attracted considerable interest because of their high T_c values and the possibility that some of them may also be half-metallic[3]. It has been reported that the addition of Co to the $Ni_{50}Mn_{37}Sn_{13}$ alloy is worth to study for several reasons: it is interesting to check how Co influences phase transitions in $Ni_{50}Mn_{37}Sn_{13}$ which exhibits large inverse MCE[4] and, second, upon substitution of Co for Ni in NiMnIn alloys, the martensitic transformation is accompanied by a marked change in the sign of exchange interactions[5].

With respect to Co-containing samples, it must be noted the fact that structural instability and exchange interactions strongly depend on the relative amount of Co. In the case of substitution of Mn by Co ($Ni_{50}Mn_{37-x}Co_xSn_{13}$), both martensitic transformation and magnetic transition temperatures exhibit minor changes with the addition of Co in place of Ni[6]. With a higher Co content, the martensitic transformation was not observed down to liquid nitrogen temperature. Results of several studies of Co-alloyed Ni(Co)-Mn-Ga revealed that the martensitic transformation temperature decreases and T_c increases upon such a substitution[6]. However, ferromagnetic ordering temperatures in Co-based Heusler systems (Co_2MnIn) are considerably higher than in the corresponding Ni_2MnIn ones[6, 7].

In addition, the ferromagnetic Heusler alloys attracted much attention owing to their peculiar magnetic and magneto-volume properties: Ni_2MnGa is considered as Ferromagnetic Shape Memory Alloys (FSMA) that emerge as active materials due to their large magnetic

field induced strain and are suitable for construction of novel actuators and sensors. A large magnetic field induced strain has been reported in Ni_2MnGa crystalline alloy with rapid response to magnetic field and readily change the shape rather than to other conventional driving forces (e. g. temperature and stress). On the contrary, the key factor of the FSMA is that the drive frequency increases enormously when the high temperature austenitic parent phase is transformed into low temperature martensite phase (Cubic-Tetragonal) by applying magnetic field. Several FSMA have been reported, among others, in Ni-Mn-Al[8] and Ni-Co-Ga[9] alloy systems. Nowadays, significative studies focused on the magnetic refrigeration around room temperature (RT) are being carried out. An important point is the search and study of new materials presenting giant MCE associated to a First Order Magnetostructural Transformation[10, 11]. It must be noted that these compounds presenting high MCE frequently show a big thermal hysteresis, which is not desirable for competitive commercial refrigeration because it must operate at frequencies of around 50 Hz[12].
In the present paper we investigate the structural and magnetic properties of ribbon samples of Heusler alloy family of compositions susceptible of exhibiting MCE and we have focused on the chemical composition $Co_{50}Mn_{30}In_{15}Sn_5$.

2. EXPERIMENTAL

The adequate quantities of the three elements corresponding to the chemical composition of the sample were melted in a Edmund Buehler (MAM-1) arc melter in order to get the master alloy in bulk. This alloy was melt spun in order to obtain the sample under ribbon-like geometry.
Differential Scanning Calorimetry (DSC) measurements were carried out in a SETARAM DCS131 calorimeter under Ar atmosphere between room temperature (RT) and 973 K at heating and cooling rates of 5 K/min. X-ray diffraction (XRD) measurements were made in a powder diffractometer of BRUKER (D8 Advance) at RT with CuKα wavelength and the JCPDS crystallographic data base was used to identify the existing phases in the material. The microstructures of the ribbons as well as the compositions analysis was performed through Scanning Electron Microscopy (SEM, JEOL 6100), equipped with an Energy Dispersive X-ray microanalysis system (EDX, Inca Energy 200). Magnetic properties (Magnetization and Hysteresis loops) of the sample were measured with PPMS (QUANTUM DESIGN Inc.) by using the

Vibrating Sample Magnetometer (VSM) technique between 15 K and 960 K with applied magnetic field ranging from 50 Oe up to 30 KOe, always with the applied magnetic field parallel to the ribbon's surface along the ribbon's axis.

The sample was measured in different states, which are: a) as-cast, b) short time (10 min.) annealing at 960 K in the PPMS under Ar atmosphere and c) long time (5 h.) annealing in a separate oven at 923 K in vacuum condition.

3. RESULTS AND DISCUSSION

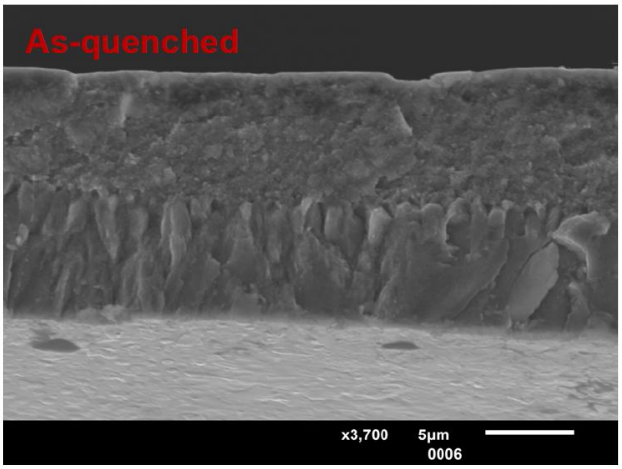

Fig. 1: SEM micrographs of as-quenched $Co_{50}Mn_{30}In_{15}Sn_5$ alloy ribbon.

Fig. 1 shows SEM images for as-quenched treatment on Co-Mn-In-Sn ribbon. In this figure, it is observed holes and small grains for as-cast ribbon. After exhaustive study by EDS microanalysis on the transversal section of the ribbons, it was shown an averaged composition about $Co_{53.2}Mn_{25.7}In_{15.5}Sn_{5.6}$ for as-quenched ribbon.
Fig. 2 shows the DSC scans for the as-cast $Co_{50}Mn_{30}In_{15}Sn_5$ ribbons. In heating curve the main recrystallization peak is observed at 820 K and other lower peaks occur at lower and higher temperature sides between 520 K and 950 K, denoting that the recrystallization process is very complex. This complexity is supported by the XRD results, whose scan for as-cast and long time annealed samples are shown in Fig. 3.

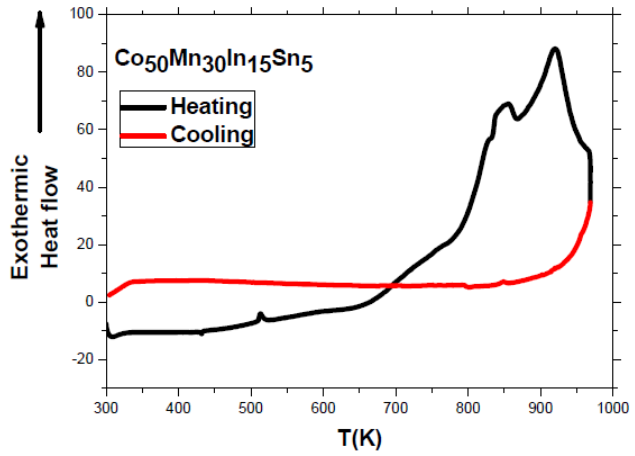

Figure 2: DSC cycles scans for the alloy $Co_{50}Mn_{30}In_{15}Sn_5$ at heating and cooling rate of 5K/min.

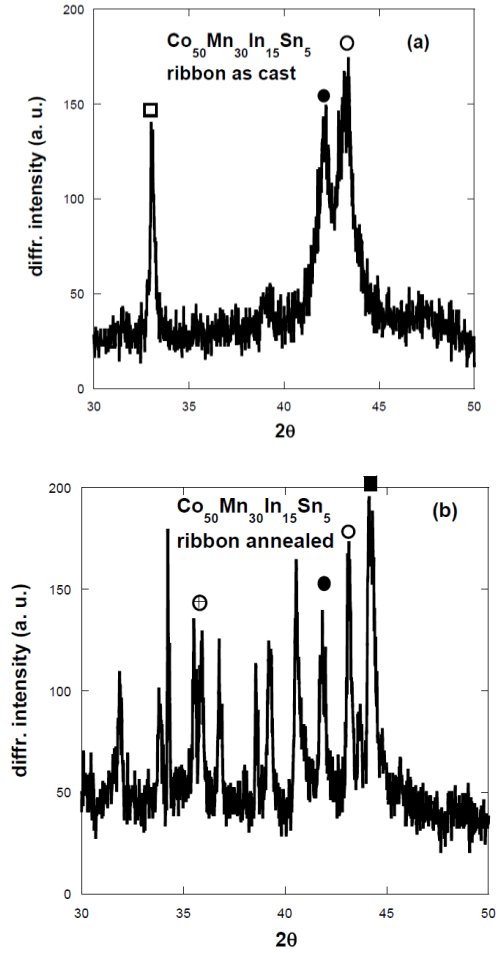

Fig: 3. - XRD scans obtained at RT for as-cast (a) and annealed (b) ribbons. In (□), Co (■), Mn (○), Co_2MnSn (●) and $CoMnIn_4$ (+) peaks have been signaled.

XRD pattern for as-cast sample show the presence of, mainly, In, Mn and Co_2MnSn crystalline phases and an overlapping amorphous halo which can be attributed to a high quantity of amorphous Co still non crystallized. After a long time annealing 960 K, the amorphous halo and the In peak disappear in the XRD pattern and the Co and Co_2MnSn phases are more intense (this is why it can be deduced that the majority of Co was not crystallized) and, among others, new $CoMnIn_4$ phase appears now. Therefore, we can say that the recrystallized ribbon is formed by multiple crystalline phases, among them Co and the Heusler one, Co_2MnSn, can be signaled. It is important to point out that 33 nm size was obtained for Co_2MnSn crystals, in the case of the annealed sample, from Scherrer's formula[13] after correction of the experimental broadening with a big crystallite standard. On the contrary, crystal size of the as-cast ribbon shows a size of some 11 nm.

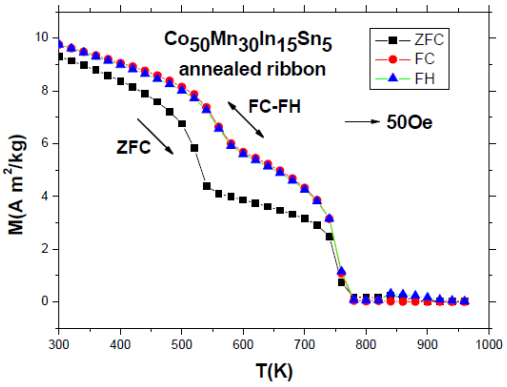

Fig.4. - Zero Field Cooling (ZFC), Field Cooling (FC) and Field Heating (FH) thermomagnetic curves for $Co_{50}Mn_{30}In_{15}Sn_5$ annealed ribbon obtained under an applied magnetic field of 50 Oe.

Fig.4 shows the thermomagnetization curves obtained for the long time annealed ribbon measured at 50 Oe. ZFC-FC-FH curves obtained at different magnetic fields (1 kOe, 10 kOe and 30 kOe) denote the same behavior in all the cases. An evident peak is observed in the three scans in the 800-900 K temperature regions, which coincides with the recrystallization measured by DSC. In addition, two different cuire temperatures are observed (Tc=500K & Tc =720K).Moreover, thermal dependence measurements of the magnetization of the as-cast sample under different applied fields also show a prominent peak in the same temperature region. This high temperature peak is not present when magnetization of the sample is measured in a second run that is after the sample is short time annealed (see Fig. 5). In this case the Curie temperature (Tc=450K) is lower than the annealed ribbon.

ICME11-RT-023

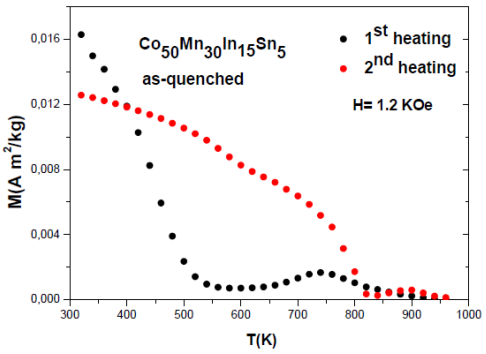

Fig. 5.- Magnetization vs. temperature plot obtained under 1.2 kOe external magnetic field for $Co_{50}Mn_{30}In_{15}Sn_5$ in two consecutive temperature runs: the first run corresponds to the as-cast ribbon and the second one to the short time annealed ribbon.

It is obvious that the T_C increase after annealing for the sample $Co_{50}Mn_{30}In_{15}Sn_5$ alloy. As we know, the heat treatment, involving stress relaxation, may decrease the strain energy. In the sample with small grain sizes, the strain energy becomes large, and thus the large driving force is required for the transformation. On the other hand, the atom site in melt spun ribbons may not be stable, since they are prepared by the quick transition from the liquid to the solid state, and do not take up an equilibrium position, in which they would have lower energy. After annealing, the melt spun ribbons undergo structural relaxation [14]. So the effect of annealing on the T_C in $Co_{50}Mn_{30}In_{15}Sn_5$ ribbons should be ascribed to the stress and structural relaxation [15].

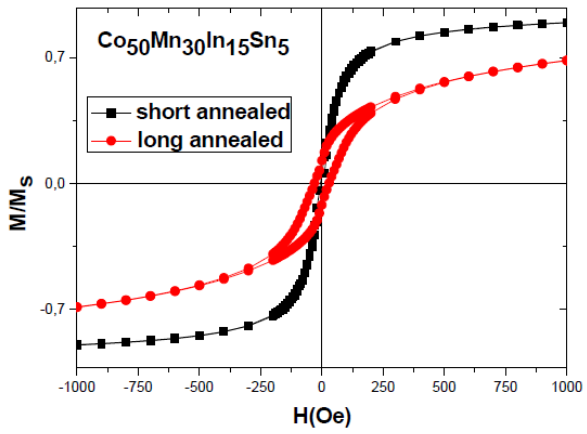

Fig. 6.- Hysteresis loops obtained for $Co_{50}Mn_{30}In_{15}Sn_5$ short and long time annealed ribbons obtained at RT.

Magnetization is normalized to the saturation magnetization of each sample.

Consequently, it is reasonable to assume that this temperature region represent for the sample a first order magnetostructural transformation, which gives the expectation of getting valuable MCE.

On the other hand, we will now focus on the hysteresis loop behaviour of the short and annealed ribbons. Fig. 6 shows hysteresis loops measured at RT for the two kinds of investigated ribbons in this work. Clear observed changes of the hysteresis loops denoting soft-hard magnetic character of the sample are inferred by the high temperature annealing: the short time annealed ribbon shows soft ferromagnetic behaviour and the long time annealed one show small increasing magnetic hardness. Moreover, the hysteresis behaviour has been also measured at 400 K and 500 K. In these cases the changes in Hc go in the same direction (the annealed ribbons are magnetically harder than the as-cast one) but the relative changes in Hc are not so important as well as its almost constant value. It is newly an indication of the complexity of the magnetostructural phase transformation of the ribbon.

The magnetic entropy change (ΔS_M) is calculated from the isothermal magnetization curves (figure 7) using the Maxwell relation:

$$\Delta S_M(T,H) = \int_{H_1}^{H_2}\left(\frac{\partial M(H,T)}{\partial T}\right)_H dH \approx \int_{H_1}^{H_2}\frac{\Delta M}{\Delta T}dH, \qquad (1)$$

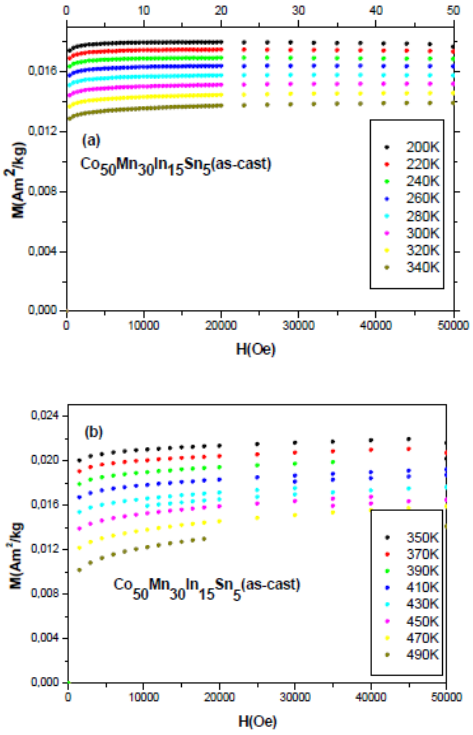

Figure 7. Isothermal magnetization curves for $Co_{50}Mn_{30}In_{15}Sn_5$ as cast ribbon.

The ΔS_M values estimated at different temperatures in $Co_{50}Mn_{30}In_{15}Sn_5$ alloy for as cast and glass annealed samples are plotted in figures 8 and 9 respectively. Figure 8 shows the entropy change (ΔS_M) in the vicinity of the second order transition temperature (SOT) for applying three different magnetic fields of 5T, 4T, and 3T for $Co_{50}Mn_{30}In_{15}Sn_5In_{15}$ as cast sample. According to equation (1) we can observe that the change of maximum entropy is decreased with increase the applied magnetic field for both as cast and annealed samples.

It is also observed that the maximum ΔS_M is found to be 2.37 J/kgK, 1.87 J/Kg K and 1.34 J/Kg K at 490 K in the magnetic fields of 5T, 4T and 3T respectively in the vicinity of SOT. It is observed that the maximum entropy change at temperature 490 K which is more or

less close to the Curie temperature (450K) for this alloy, that we have discussed by M versus T measurements in this paper. However, the ΔS_M is found to decrease almost linearly with external magnetic field. It can be seen that the value of ΔS_M decreases evidently with increasing ΔH. Furthermore, it is observed that for the field of 5T the maximum ΔS_M is 2.37 J/Kg K which is comparable with the most well known compound of Gd_5Si_4 [16] with $\Delta S_{M=}$ 9 J/Kg K at temperature 336K and 8.2 J/KgK at temperature 345.7K [17].

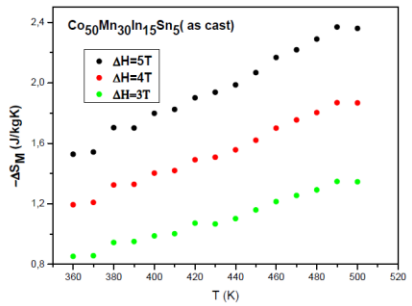

Figure 8. Magnetic entropy change (ΔS_M) in $Co_{50}Mn_{30}In_{15}Sn_5$ (as-cast) alloy with temperature under the fields of 5T, 4T and 3T.

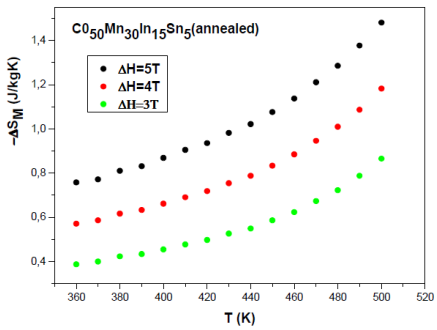

Figure 9. Magnetic entropy change (ΔSM) in $Co_{50}Mn_{30}In_{15}Sn_5$ (annealed) alloy with temperature under the fields of 5T, 4T and 3T.

Figure 9 shows the entropy change (ΔS_M) in the vicinity of the SOT for applying three different magnetic fields of 5T, 4T, and 3T for $Co_{50}Mn_{30}In_{15}Sn_5$ annealed sample. However, we find very similar behaviour to the obtained one for the as cast sample. Furthermore, it is observed that the maximum entropy change is going to the higher temperature range which could be more than 1000K. It is worth noting that we were not able to measure it more than 1000K temperature range and for this case we did not calculate MCE effect for this annealed sample.

4. CONCLUSION

The structural and magnetic measurements carried out on as-cast and high temperature annealed $Co_{50}Mn_{30}In_{15}Sn_5$ ribbons show a very complex magnetostructural transformation occurs in the 800-900 K temperature regions. The Heusler Co_2MnSn is present in all the cases, but in greater quantity when the sample is annealed which is three times greater than the as cast ribbon. We also studied the magnetic entropy change of this alloy. It shows the highest ΔS_M value of 2.37 J/Kg K for a field change of 5T.This fact leads us to expect that this composition (or different compositions based in lower quantities of Co and/or In) will present good conditions in order to get valuable magnetocaloric effect results. This work is now in progress.

ACKNOWLEDGEMENTS

Authors are thankful to Spanish MICINN for financial support: MAT2009-13108-C02-01-02 and MAT2010-20798-C05-04.M.Nazmunnahar thanks to Basque government for a grant. L. González also thanks to MICINN for a FPI grant and J. García to FICYT for a "Severo Ochoa" grant.

5. REFERENCES

1. A. M. Tishin and Y. Spichkin, *The magnetocaloric effect and its applications*, Institute of Physics Publishing, Bristol (2003).

2. V. K. Pecharsky and K. A. Gschneidner Jr, J. Magn. Magn. Mat. 200**,** 44 (1999).

3. S. Ishida, T. Masaki, S. Fujii and S. Asano, Physica B 245 (1998).

4 .T. KrenKe, E. Duman, M. Acet, E. F. Wassermann, X. Moya, L. Manosa and A. Planes, Nature Mater. 4, 450 (2005).

5 .R. Kainuma, Y. Imano, W. Ito, Y. Sutuo, H. Morito, S. Okamoto, O. Kitakami, K. Oikawa, A. Fujita, T.Kanomata and K. Ishida, Nature 439, 957 (2006).

6 .V. Khovaylo, V. Koledov, V. Shavrov, M Ohtsuka, H. Miki, T. Takagi and V. Novosad, Mat.Sci. Eng. A418-482, 322 (2008).

7 .V. Sánchez-Alarcos, J. I. Pérez-Landazábal, V. Recarte, C. Gómez-Polo, J. A. Rodríguez-

Velamazán, Acta Mat.56, 5370 (2008).
8 .K. Oikawa, L. Wulff, T. Iijima, F. Gejima, T. Ohmori and K. Ishida, Appl. Phys. Lett. 79, 3290 (2001).
9 .K. Oikawa, T. Ota, T. Ohmori, H. Morito, A. Fujita,Y. Tanaka and K. Ishida, Appl. Phys. Lett. 81, 5201 (2002).
10. H. Wada and Y. Tanabe, Appl. Phys. Lett.79, 3303 (2001).
11. O. Tegus, E. Bruck, K. H. J. Buschow and F. R. de Boer, Nature **415**, 450 (2002).
12.E. Bruck, J. Phys. D: Appl. Phys.**38**, 381 (2005).
13. H. P. Klug and L. E. Alexander, *X-ray diffraction procedures for polycrystalline and amorphous materials*, Wiley, New York (1974).
14. H.C. Xuan, K.X. Xie, D.H. Wang, Z.D. Han, C.L. Zhang, B.X.Gu, and Y.W, Appl. Phys. Lett.**92** (2008).
15. D.H Wang, K.Peng, B.X.Gu, Z.D. Han,S.L.Tang, W.Qin, and Y.W.Du, J. Alloys Compd. **358** (2003) 312.
16. Gschneidner K. A. Jr and Pecharsky V. K, J. Appl. Phys. **85** (1999) 5365.
17. Spichkin Y. I, Pecharsky V. K and Gschneidner K. A. Jr, J. Appl. Phys. **89** (2001) 1738.

7. NOMENCLATURE

Symbol	Meaning	Unit
T	Temperature	(K)
M	Magnetization	(A m^2/kg)
H	Magnetic field	(A/m)
T_c	Curie temperature	(K)